NIH Public Access
Author Manuscript
Neurobiol Aging. Author manuscript; available in PMC 2013 July 1.

Published in final edited form as:
Neurobiol Aging. 2012 July ; 33(7): 1273–1283. doi:10.1016/j.neurobiolaging.2010.12.007.

Combination therapy prevents amyloid-dependent and –independent structural changes

Gauri Malthankar-Phatak[a], **Shane Poplawski**[b], **Nikhil Toraskar**[a,1], and **Robert Siman**[a]

Gauri Malthankar-Phatak: gaurangi@mail.med.upenn.edu; Shane Poplawski: shanepop@mail.med.upenn.edu; Nikhil Toraskar: ntatupenn@gmail.com; Robert Siman: siman@mail.med.upenn.edu

[a]Department of Neurosurgery, University of Pennsylvania School of Medicine, Philadelphia, PA 19104

[b]Department of Pharmacology, University of Pennsylvania School of Medicine, Philadelphia, PA 19104

Abstract

Neuropathological features of Alzheimer's disease (AD) are recapitulated in transgenic mice expressing familial AD-causing mutations, but ectopic transgene overexpression makes it difficult to relate these abnormalities to disease pathogenesis. Alternatively, the APP/PS-1 double knock-in mouse (DKI) produces mutant APP and PS-1 with normal levels and regulatory controls. Here, we investigated effects of amyloid on brain structure and neuroplasticity by vaccinating DKI mice with amyloid-β starting at 8 months of age. At 14 months, vaccination blocked cerebral amyloid deposition and its attendant microglial activation. Neuropil abnormalities were pronounced only within plaques, and included circumscribed loss and dysmorphology of axons, dendrites, terminals and spines. Blockade of amyloid deposition restored neuropil integrity. Amyloid removal did not rescue reductions in the hippocampal neural progenitor and neuroblast populations, but adding one month of voluntary exercise to amyloid-β vaccination markedly stimulated hippocampal neurogenesis. These results identify amyloid-dependent and –independent structural changes in the DKI mouse model of AD. Combining exercise with amyloid-directed immunotherapy produces greater restoration of brain structure and neuroplasticity than is achieved with either maneuver alone.

Keywords

Aβ vaccination; voluntary exercise; dystrophic neurites; neurogenesis; synapse loss; knock-in mouse; Alzheimer's Disease; combination therapy; neuroplasticity

© 2010 Elsevier Inc. All rights reserved.

Corresponding Author: Robert Siman PhD, University of Pennsylvania School of Medicine, Department of Neurosurgery, 502E Stemmler Hall, 36th and Hamilton Walk, Philadelphia, PA 19104; siman@mail.med.upenn.edu. Telephone: (215) 573-6245; Fax: (215) 898-9217.

[1]Present address: Aderans Research, 3401 Market Street Suite 318, Philadelphia, PA 19104

Publisher's Disclaimer: This is a PDF file of an unedited manuscript that has been accepted for publication. As a service to our customers we are providing this early version of the manuscript. The manuscript will undergo copyediting, typesetting, and review of the resulting proof before it is published in its final citable form. Please note that during the production process errors may be discovered which could affect the content, and all legal disclaimers that apply to the journal pertain.

Disclosure statement: There are no conflicts of interest for any of the authors.

NIH-PA Author Manuscript
NIH-PA Author Manuscript
NIH-PA Author Manuscript

NIH-PA Author Manuscript

NIH-PA Author Manuscript

NIH-PA Author Manuscript

1. Introduction

Excepting its early age of onset, familial Alzheimer's disease (AD) resembles the sporadic form of the disease in its clinical signs, slow progression, and characteristic aging- and brain region-dependent neuropathologies and neurodegeneration. Many of the neuropathological features of AD can be recapitulated in mouse models transgenic for familial AD-causing mutations in the genes for amyloid precursor protein (*APP*), presenilin-1 (*PS-1*), or bitransgenics expressing both mutant *APP* and *PS-1*, including cerebral amyloid deposition, reactive gliosis, neuritic dystrophy and synapse loss. However, there is disagreement over the extent and mechanisms of neuronal atrophy and degeneration in the various transgenic lines. Some studies report extensive loss of nerve terminal, dendritic, and dendritic spine markers across the forebrain, in some cases even before the onset of cerebral amyloid pathology (Hsia et al., 1999; Lanz et al., 2003; Buttini et al., 2005), whereas others describe circumscribed disruption of the neuropil restricted to amyloid plaques (Le et al., 2001; Tsai et al., 2004; Spires et al., 2005). This unresolved issue is especially important in light of evidence that neocortical synapse loss is the strongest neuropathological correlate of cognitive impairment of AD (Terry et al., 1991).

There are two major neurogenic systems in the adult mammalian brain, and considerable evidence implicates newborn dentate granule neurons in at least certain forms of hippocampus-dependent learning and memory (Dupret et al., 2008; Deng et al., 2009; Kitamura et al., 2009). Investigations of the fidelity of hippocampal neurogenesis in mouse transgenic models of AD have yielded divergent results (Wen et al., 2002; Jin et al., 2004; Donovan et al., 2006; Verret et al., 2007; Kolecki et al, 2008), and any relationship between the amyloid pathology and neurogenesis remains poorly defined.

Unfortunately, the ectopic overexpression of APP and PS-1 transgenes complicates mouse studies of the progressive pathogenic mechanisms of AD, as it has the potential to trigger structural and functional abnormalities unrelated to the disease process. For example, the degree to which transgenic expression of mutant APP and PS-1 models the neural circuit and behavioral dysfunction of AD is difficult to ascertain, since even wild type transgene overexpression elicits cellular, anatomical, physiological, and behavioral disturbances (Mucke et al., 1994; Thinakaran et al., 1996; Nalbantoglu et al., 1997; Wen et al., 2002; Auffret et al., 2009; Naumann et al., 2009). In addition, although transgenic mouse models have played an essential role in the development of immunotherapeutic approaches for AD, transgenic APP overexpression leads to tolerization of mice toward amyloid β-vaccination that would not be expected in the AD patient (Monsonego et al., 2001). As an alternative, we introduced a gene-targeted mouse model bearing familial AD-causing point mutations in its endogenous *APP* and *PS-1* genes (Reaume et al., 1996; Siman et al,, 2000; 2001). The APP/PS-1 double knock-in mutant mouse (DKI) develops progressive amyloid deposition and reactive gliosis in brain regions vulnerable in the human disease (Flood et al., 2002; Siman and Salidas, 2004). Furthermore, the DKI mouse has a long-lasting reduction in adult hippocampal neurogenesis (Zhang et al., 2007). Thus, the DKI mouse provides a model for evaluating the extent and mechanisms of degenerative and neuroplastic changes in the absence of transgenic overexpression, and identifying therapeutic approaches for reducing AD-type pathologies. In the current study, we characterized the spectrum of neuronal atrophy and degeneration in the DKI mouse, and evaluated the efficacy of Aβ vaccination both alone and as part of combination therapy aimed at preventing structural abnormalities and the loss in neuroplasticity.

NIH-PA Author Manuscript

NIH-PA Author Manuscript

NIH-PA Author Manuscript

2. Materials and methods

2.1. The APP/PS-1 DKI mouse line

The APP/PS-1 double knock-in mutant mouse line was created using gene targeting in embryonic stem cells, and has been described and characterized extensively before (Reaume et al., 1996; Siman et al., 2000; 2001; Flood et al., 2002; Siman and Salidas, 2004). The mouse APP gene carries the Swedish double point mutation at codons 670–671, and the three variant codons within the Aβ domain have been changed from the mouse to the human sequence. The mouse PS-1 gene carries the FAD-linked P264L point mutation. The DKI mouse line is homozygous for the two mutant alleles for both genes. Mice were given free access to food and water, and maintained under veterinary supervision in strict compliance with all standards for animal care and investigation established in the "Guide For The Care And Use Of Laboratory Animals" (National Academy Press ISBN# 0-309-05377-3). Both male and female mice were used for all studies.

2.2. Experimental design

The effects of amyloid deposition on neuropil integrity and neurogenesis were evaluated using two different therapeutic approaches, anti-Aβ immunotherapy and voluntary exercise. The first involved vaccinating DKI mice with Aβ starting at 8 months of age. The mice in this group (n=14) were used for histology at 15 months of age, ~3 weeks after their final immunization. Age- and gender-matched DKI shams receiving incomplete Freund's adjuvant injections starting at 8 months of age were used as controls (n=6) along with wild-type mice (n=12). The second involved voluntary exercise using running wheels, either in combination with the Aβ vaccination or alone. The mice were given unlimited access to running wheels for 30 days starting immediately after receiving their final immunization (at 14 months of age) and used for histological evaluation at the end of the running period (15 months of age; n=9). Age- and gender-matched sedentary DKI mice served as controls (n=12). An additional group of non-vaccinated DKI mice were evaluated for histology after being given access to running wheels for 30 days starting at 14 months of age (n=6). Both male and female mice were studied throughout and the data were pooled for final analyses due to the lack of effect of gender on the results.

2.3. Amyloid-β vaccination

Synthetic human Aβ1-42 (Bachem, King of Prussia, PA) was solubilized, pre-aggregated, and emulsified in complete Freund's adjuvant as described before (Games et al., 2000; Wilcock et al., 2001). The resulting emulsion was injected subcutaneously into each mouse at two sites (100 μg Aβ per mouse) starting at eight months of age. Every 5–6 weeks thereafter for 6 months, each mouse received booster injections of 25 μg Aβ1-42 emulsified in incomplete Freund's adjuvant. The first three boosts were delivered subcutaneously, and subsequent immunizations were intraperitoneal. The mice receiving Aβ vaccination without voluntary exercise were euthanized 2–3 weeks after their final immunization. Non-vaccinated wild type and DKI mice matched for age and gender were processed for histology at the same time.

2.4. Voluntary exercise

At the end of the 6-month vaccination period, some cohorts of mice were given unlimited access to a running wheel for 30 days. The distance run per day was monitored using counters fitted with a magnetic sensor (Readington Counters, Windsor, CT) attached to the running wheels. The mice were prepared for histology at the end of the 30-day exercise period. Groups of age- and gender-matched non-vaccinated sedentary wild type and DKI mice served as controls.

NIH-PA Author Manuscript

NIH-PA Author Manuscript

NIH-PA Author Manuscript

2.5. Immunocytochemistry and morphometry

At the end of their respective treatment periods, mice were anesthetized deeply with an overdose of pentobarbital, then perfused transcardially with ice cold 0.1M sodium phosphate buffer at pH 7.4 (PB), followed by ice cold freshly prepared 4% paraformaldehyde in PB. Brains were carefully dissected, post-fixed for 4 hours at 4°C, cryoprotected in 20% sucrose in PB overnight, blocked, frozen, and stored at −80°C. Sagittal 40 μm sections were prepared with a sliding microtome and collected sequentially into ten series, with each starting from the medial border of hippocampus and extending laterally to the start of the ventral hippocampus. The total number of sections between these anatomical boundaries did not differ as a function of APP or PS-1 genotype, or following Aβ vaccination with or without voluntary exercise.

A minimum of two series of sections (at least 10 sections) were immunostained by an indirect immunoperoxidase method either for doublecortin (Santa Cruz Biotechnologies, 1/1000 dilution), a marker for immature neurons (Nacher et al., 2001; Rao and Shetty, 2004), Ki-67 (Epitomics, Burlingame, CA, 1/2000 dilution), a marker for dividing neural stem/progenitor cells (Gerdes et al., 1983), spinophilin (Millipore, Bellerica, MA; 1/2000 dilution), synaptophysin (Millipore, Bellerica, MA; 1/10,000 dilution) or amyloid Aβ (Ab1153 at 1/10,000 dilution; Savage et al., 1994; Siman and Salidas, 2004). For avidin-biotin immunoperoxidase staining, sections were treated as described previously (Roberts-Lewis et al., 1994; Siman and Salidas, 2004). When required, sections were lightly counterstained with hematoxylin after being slide mounted. Some sections were counterstained for fibrillar amyloid deposits using thioflavin S at 0.1%. Photomicrographs were captured under brightfield and Nomarski illumination on a Nikon Eclipse E600 microscope outfitted with a Nikon DXM-1200 camera. The images of the sections stained with thioflavin-S were captured using a cooled CCD monochromatic camera.

The amyloid Aβ burden in dorsal hippocampus within the mediolateral boundaries described above was determined by selecting as region of interest the entire hippocampus bordered by the alveus (dorsal), the lateral ventricle (ventral), and the subiculum (caudal). Amyloid deposition was quantified by binary thresholding and calculating the percentage of hippocampal area occupied by the Aβ. The numbers of Ki-67-immunopositive neural stem/progenitor cells and doublecortin-immunopositive immature neurons in the subgranular zone of the dentate gyrus were counted by an observer blinded to the treatment group under brightfield illumination at 400X magnification. Both blades of the subgranular zone were evaluated along their entire rostro-caudal axis starting at the medial border of dorsal hippocampus and extending laterally to the start of ventral hippocampus. Because of the small numbers of stained cells, all possible labeled cells within the chosen anatomical boundaries were counted adhering to the rare event protocol sampling scheme of unbiased stereology (Mouton, 2002). Labeled cells are represented as the total number of immunostained cells per dorsal hippocampus, and compared with the number of immunopositive cell from APP/PS-1 wild type mice. A minimum of 100 immunopositive cells were counted for each marker and mouse brain.

Antibodies to the following proteins were used to stain one series of sections each by indirect immunofluorescence: amyloid Aβ1-28 (Ab1153 at 1/5000 dilution), MAP2 (Santa Cruz Biotechnologies; 1/400 dilution), a hypophosphorylated form of neurofilament H (pNFH; SMI-35 from Millipore; 1/2000 dilution), synaptophysin (Millipore; 1/3000 dilution), and CR3/cd11b (AbDSerotec, Raleigh, NC; 1/200 dilution). For immunofluorescence microscopy, slide-mounted sections were treated with autofluorescence quencher (Chemicon, Bellerica, MA) for 1.5 minutes, then permeabilized and pre-blocked with TBS containing 0.05% Triton X-100 and 3% normal goat serum for 1 hour at room temperature. Sections were incubated in primary antibodies followed by goat

NIH-PA Author Manuscript

NIH-PA Author Manuscript

NIH-PA Author Manuscript

anti-rabbit, anti-rat, or anti-mouse secondary antibodies conjugated to AlexaFluor-488 or -568 (Molecular Probes, Carlsbad, CA; 1/500 dilution). Sections were washed, coverslipped using Vectashield with DAPI (Vector Laboratories) and stored in the dark at 4°C. Microscopic images were captured in 8–12 z-steps of 1 μm using NIS-Elements imaging software and a cooled CCD monochromatic camera. The z-stacks were deconvolved using the autoquant algorithm of NIS-Elements and saved as maximum intensity projection two-dimensional images compiled from digitally sectioned z-planes. Each experiment labeled and analyzed sections derived from both control and treated groups to ensure internal experimental consistency. All images for a given immunostain were taken using the same exposure time, deconvolved using equivalent settings, and prepared for publication using equivalent processing methods in Photoshop.

2.6. Statistical analyses

All bar graphs show the mean +/− SEM. The numbers of doublecortin-positive immature neurons and Ki-67-positive dividing stem/progenitors were compared across experimental groups using Student t-test with *a priori* value of 0.05 as well as ANOVA.

3. Results

3.1 Effects of Aβ vaccination on amyloid deposition in the DKI mouse

With the objective of evaluating the contribution of amyloid deposition to any neurodegenerative, atrophic or neuroplastic changes in the APP/PS-1 double knock-in (DKI) mouse model of AD, we first explored active immunization with human Aβ1-42 as a means of blocking cerebral amyloid deposition. Vaccinations with Aβ were begun at 8 months of age, about 2 months after amyloid deposition and reactive gliosis are first detectable in regions of the neocortex and hippocampus (Flood et al., 2002; Siman and Salidas, 2004). In 14 month-old DKI mice not receiving any Aβ vaccinations, amyloid deposition was restricted to the telencephalon, and was extensive within gray matter in the neocortex and hippocampal formation. Immunostaining with an antibody directed at Aβ1-28 revealed large numbers of amyloid deposits of various sizes and morphologies in the outer molecular layer of dentate gyrus, subiculum (Fig. 1A), and layers I–V of frontal, parietal, and temporal neocortex. This antibody is directed against amyloid aggregates, does not label APP and does not produce intracellular staining. It labels both fibrillar and diffuse plaques that are abundant in the brain parenchyma of AD patients as well as our DKI and other mutant rodent models (Siman et al., 2000; Flood et al., 2002; Siman and Salidas, 2004; Flood et al., 2009). We also performed Thioflavin S staining, which confirmed that some deposits were fibrillar core-containing amyloid plaques (Fig. 1C). In sharp contrast, following 6 months of Aβ vaccination the neocortex and hippocampal formation at 14 months of age were virtually devoid of amyloid deposits (Fig. 1B). The failure to label amyloid deposits following Aβ vaccination was not simply an artifact of epitope masking by endogenous Aβ antibodies, since thioflavin S-positive fibrillar amyloid plaques also were blocked by the vaccination (Fig. 1D). Quantitative morphometric analysis of the area occupied by amyloid deposits revealed that 6 months of Aβ vaccination led to a 97% reduction in amyloid burden in dentate gyrus (Fig. 1E). There were no instances of microhemorrhage or cerebrovascular amyloid accumulation after Aβ vaccination. Thus, in the DKI mouse that does not over express APP and so is not tolerized to the Aβ protein, vaccinations with human Aβ1-42 are extremely effective at preventing cerebral amyloid deposition.

3.2. Neuropil Disruption within plaques and effects of Aβ vaccination

To assess the Alzheimer-type neuronal atrophy and degeneration in the DKI mouse and evaluate any deleterious effects of amyloid deposition, an array of markers was used to discern the integrity of dendrites, axons, and synapses at 14 months of age, a time when

NIH-PA Author Manuscript

NIH-PA Author Manuscript

NIH-PA Author Manuscript

cerebral amyloid deposition is already extensive. MAP2 immunolabeling (Fig. 2A, shown in green) revealed dense networks of dendrites in neocortex and hippocampus, with focal areas of dendritic disruption confined to the circumscribed amyloid deposits co-immunolabeled for Aβ (Fig. 2A, shown in red). In contrast, in areas of neocortex and hippocampus devoid of amyloid deposits the density of MAP2 immunostaining did not differ between wild type and DKI mouse brain. Prior studies have reported that dendritic morphology is aberrant surrounding amyloid deposits, abnormalities that have been referred to as curvy dendrites (Knowles et al., 1999;Le et al., 2001). Under high magnification, curvy dendrites immunostained for MAP2 were associated with the periphery of amyloid deposits in the DKI mouse forebrain (Fig. 2C), and in many cases formed an annulus around the Aβ. Aβ vaccination was effective not only at blocking cerebral amyloid deposition, but it also prevented both the focal loss of dendrites and the appearance of curvy dendrites (Fig. 2B,D).

To determine whether the circumscribed neuropil disruption within amyloid deposits involved other neuropil constituents, neurofilament H immunostaining was used to assess axonal integrity. The SMI-35 monoclonal that labels a hypophosphorylated form of neurofilament H expressed predominantly in axons (Sternberger and Sternberger, 1983) revealed the presence of enlarged axonal varicosities and loss of normal axons in association with amyloid deposits in the DKI mouse neocortex and hippocampus (Fig. 3B), but not in wild type mouse brain (Fig. 3A). This axonopathy was blocked by Aβ vaccination (Fig. 3C), providing evidence that amyloid deposits disrupt axons as well as dendrites.

To evaluate the effects of amyloid deposition on synapse integrity in the DKI mouse model, we immunostained dendritic spines for spinophilin and pre-synaptic terminals for synaptophysin. Spinophilin immunoreactivity was present in a dense plexus of small puncta throughout the dentate molecular layer (Fig. 4A), as expected for its distribution within dendritic spines. Conspicuously, spinophilin was absent in circumscribed spheres (asterisks) that were confirmed by double labeling as thioflavin S-positive amyloid plaques (Fig. 4B). Blockade of amyloid deposition by Aβ vaccination prevented the focal loss of the dendritic spines (Fig. 4C), and the dense plexus of spines was interrupted only by blood vessels traversing the molecular layer (arrows). Similar to spinophilin-positive spines, synaptophysin-positive nerve terminals also formed a dense array of small puncta in the dentate molecular layer of the wild type mouse (Fig. 4D), but in the molecular layer of the DKI mouse spherical areas containing swollen nerve terminals and devoid of the small immunoreactive puncta were associated with amyloid deposits (Fig. 4E). Once again, Aβ vaccination prevented the focal loss of synaptophysin-positive terminals and the appearance of swollen nerve endings (Fig. 4F). An axonal source for the dystrophic neurites associated with amyloid plaques was confirmed by co-localization of synaptophysin-positive swellings with fibrillar amyloid plaques labeled with thioflavin S (Fig. 4G,H).

Finally, the effects of amyloid deposits on microglia were assessed by immunostaining for the marker CR3/cd11b (Graeber et al., 1988). Microglia immunopositive for CR3 are present in the dentate molecular layer of the 14-month-old DKI mouse in two distinct morphologies (Supplementary data). Relatively small and lightly stained microglia with thin, short, highly ramified processes were distributed throughout the molecular layer, as well as the rest of the telencephalon. A second, activated microglial population that was much larger, with thicker processes and strong expression of CR3 overlapped with co-labeled amyloid deposits. Blockade of amyloid deposition by Aβ vaccination also eliminated the clusters of activated microglia, although some large microglia with strong CR3 expression remained scattered throughout the molecular layer.

NIH-PA Author Manuscript

NIH-PA Author Manuscript

NIH-PA Author Manuscript

3.3. Blockade of amyloid deposition does not prevent the impairment in hippocampal neurogenesis

We reported previously that the DKI mouse exhibits a long-lasting impairment in hippocampal neurogenesis that is present around the onset of cerebral amyloid deposition and persists throughout the rest of adult life (Zhang et al., 2007). To investigate further the relationship between amyloid deposition and impaired neurogenesis, the numbers of dividing neural stem/progenitor cells and differentiating neuroblasts were measured with and without Aβ vaccination. As shown in Fig. 5, immature neurons immunostained for the marker doublecortin (Nacher et al., 2001; Rao and Shetty, 2004) were localized to the neurogenic subgranular zone, with their developing dendritic arbors extending into the molecular layer. The total number of immature neurons in the dorsal dentate gyrus did not differ between 14-month-old DKI mice with extensive amyloid pathology (group NV; Fig. 5A) and those receiving 6 months of Aβ vaccination and devoid of hippocampal amyloid deposits (group V; Fig. 5B; also see Fig. 5D bargraph). We also evaluated the population of dividing neural progenitors by immunostaining for Ki-67, which is expressed exclusively in proliferating cells in late G1, S, G2 and M phases of the cell cycle (Gerdes et al., 1983). Sparse numbers of nuclei immunostained for Ki-67 were found in the neurogenic subgranular zone (Fig. 5E). Their number in the dorsal dentate gyrus also was unaffected by Aβ vaccination (Fig. 5D). Thus, reductions in the adult DKI mouse hippocampus in the neural stem/progenitor and differentiating neuroblast populations were not rescued by blocking cerebral amyloid deposition.

3.4. Combination therapy with voluntary exercise and Aβ vaccination

A well-established manipulation for promoting adult hippocampal neurogenesis is physical exercise (van Praag et al., 1999; Kempermann et al., 2000). We confirmed that 30 days of voluntary wheel running exercise starting at 14 months of age increased the number of Ki-67-positive neural progenitors and doublecortin-positive immature neurons in the subgranular zone of the dentate gyrus (data not shown). On the other hand, a 30-day period of voluntary exercise starting at 14 months of age did not appreciably affect the amyloid deposition in the DKI mouse (compare Fig. 6B to 6A). Similarly, voluntary exercise did not reverse the neuropil damage caused by the amyloid deposition, as evidenced by the continued focal loss of MAP2 staining within the deposits (Fig. 6C,D). Hence, neither immunotherapy nor voluntary exercise alone was capable of restoring both neuropil integrity and neuroplasticity.

Consequently, we investigated whether the addition of voluntary wheel running exercise to Aβ vaccination could stimulate adult hippocampal neurogenesis while retaining the beneficial effects of the vaccination on neuropil and synapse integrity. A 30 day period of exercise begun 6 months after initiating Aβ vaccination markedly increased the numbers of doublecortin-positive immature neurons (compare Fig. 5C to 5A) and Ki-67-positive dividing progenitors (compare Fig. 5F to 5E) in the dentate gyrus subgranular zone. Quantitative analysis revealed that the combination therapy increased the number of differentiating neuroblasts by almost four-fold and neural stem/progenitors by nearly three-fold (Fig. 5D). The developing new granule neurons also exhibited more extensive dendritic arborizations in the molecular layer following 30 days of wheel running exercise. The enhanced neuroplasticity induced by voluntary exercise in combination with Aβ vaccination did not interfere with the restorative effects of the vaccine on dendrites, axons, and synapses. Immunostaining for dendritic and synaptic markers was compared between DKI mice receiving the combination therapy and wild type mice. Following Aβ vaccination and voluntary exercise in DKI mice, the density of synaptophysin-positive nerve terminals did not differ appreciably from wild-type mice (Fig. 6E,F). Similarly, in DKI mice receiving the combination therapy neither the intensity of MAP2 labeling nor the dendritic density in the

NIH-PA Author Manuscript

NIH-PA Author Manuscript

NIH-PA Author Manuscript

dentate molecular layer differed from wild type mice (Fig. 6G,H). Essentially identical results were obtained in the parietal neocortex and subiculum, two other brain regions exhibiting marked amyloid deposition and neuropil disruption in the DKI mouse.

4. Discussion

This study delineates both amyloid-dependent and -independent structural changes in the DKI mouse model of AD, and identifies therapeutic strategies that ameliorate independently the two classes of structural defects. Hippocampal and neocortical amyloid deposition is accompanied by the dysmorphology and loss of dendrites, axons, and synapses. We provide strong evidence that these neuropil abnormalities are amyloid-dependent, since they occur focally in strict spatial association with amyloid deposits and are blocked by an active Aβ vaccination that virtually eliminates cerebral amyloid pathology. On the other hand, impaired neurogenesis in the adult DKI mouse (Zhang et al., 2007) can be dissociated from the amyloid pathology, as the prevention of deposition fails to increase the neural progenitor and immature neuron populations. Instead, voluntary exercise enhances adult hippocampal neurogenesis, and combines with Aβ vaccination to produce greater restoration of normal brain structure than achieved by either therapy alone. These findings have implications for understanding the progressive mechanisms contributing to AD pathogenesis and developing therapeutic strategies for protecting brain structure and neuroplasticity.

The relationship between amyloid deposition and neuropil disruption in mouse models of AD has been controversial, with transgenic studies disagreeing on the regional extent of dendritic and synaptic loss and their spatial relationship to cerebral amyloid deposition (Hsia et al., 1999; Lanz et al., 2003; Buttini et al., 2005; Le et al., 2001; Tsai et al., 2004; Spires et al., 2005). Interpretation of these studies is further complicated by the overexpression of APP and PS-1 inherent to transgenesis, since overexpression of even wild type transgenes can elicit cellular, anatomical, physiological, and behavioral abnormalities (Mucke et al., 1994; Nalbantuglo et al., 1997; Wen et al., 2002; Chang and Suh, 2005; Auffret et al., 2009; Neumann et al., 2009). These effects are unlikely to be related to the pathogenic mechanisms of AD, in which APP and PS-1 expression are not elevated (Johnson et al., 1988; Rockenstein et al., 1995; Johnston et al., 1996). In the DKI mouse model, the effectiveness of Aβ1-42 vaccination in blocking cerebral amyloid deposition (Fig. 1), coupled with the lack of any artifacts tied to transgene overexpression, facilitated the analysis of neuropil abnormalities triggered by the amyloid. The lack of APP overexpression and concomitant tolerization to Aβ immunization that results from this overexpression (Monsonego et al., 2001) is a plausible explanation for the near-complete blockade of cerebral amyloid deposition in the DKI mouse model.

Our comprehensive analyses of markers for axons, dendrites, pre-synaptic terminals and dendritic spines demonstrate that, in the absence of transgenic overexpression, amyloid deposition leads to circumscribed alterations in all these neuropil elements relatively early in the course of the disease. Dendrites expressing MAP2 are lost within plaques in the DKI forebrain, and surrounding dendrites take on an abnormal curved morphology (Fig. 2). Synapse loss also is confined to amyloid deposits, as evidenced by the circumscribed loss of both synaptophysin and spinophilin (Fig. 4). Axonal disruption develops at the periphery of amyloid plaques in the form of swollen varicosities containing both nerve terminal and axonal markers (Fig. 3). The dystrophic neurites associated with neuritic plaques in the AD brain have been thought to arise at least in part from dendrites (Grutzendler et al., 2007), but our data with compartment-specific markers argue that the plaque-associated swellings and enlarged varicosities are an axonopathy (see also Brendza et al., 2003). Finally, activated microglia with enlarged morphology and increased expression of CR3/cd11b also become clustered around amyloid deposits (Supplementary data). All of these neuropil abnormalities

NIH-PA Author Manuscript

NIH-PA Author Manuscript

NIH-PA Author Manuscript

are blocked by Aβ vaccination that eliminates cerebral amyloid deposition. Interestingly, studies of early-stage probable AD and Down's syndrome cases have provided evidence that cerebral amyloid deposition can initiate many years before the onset of clinical dementia (Mann et al., 1989;Morris and Price, 2001;Jack et al., 2010), but the role of amyloid deposition in triggering the full neuropathological spectrum of AD remains uncertain.

Adult neurogenesis is thought to contribute to certain forms of hippocampus-dependent learning and memory (Dupret et al., 2008; Deng et al., 2009; Kitamura et al., 2009), and we reported previously that the adult DKI mouse hippocampus contains reduced numbers of both dividing neural progenitors and differentiating neuroblasts (Zhang et al., 2007). These findings raise the possibility that defective hippocampal neurogenesis may be a contributing factor for cognitive decline at least in the early stages of AD, and suggest that interventions to restore this form of neuroplasticity might be of therapeutic benefit. Here we demonstrate that impaired hippocampal neurogenesis can be dissociated from amyloid deposition, as Aβ vaccination does not alter the numbers of either Ki-67-positive neural progenitor cells or doublecortin-positive immature neurons in the dentate gyrus subgranular zone (Fig. 5). Instead, the addition to Aβ vaccination of voluntary wheel running exercise, an established stimulator of neural progenitor proliferation (Van Praag et al., 1999; Kempermann et al., 2000), markedly increases neural progenitor and differentiating neuroblast populations in the DKI mouse dentate gyrus. The stimulatory effect of exercise on this form of neuroplasticity does not interfere with the beneficial effects of vaccination on the amyloid-dependent axonal, dendritic and synaptic abnormalities, whereas the one month of exercise alone fails to prevent amyloid deposition and its associated neuropil disruption (Fig. 6). The inability of active Aβ immunization to restore hippocampal neurogenesis differs from a recent result with passive immunization, in which long-term delivery of an Aβ antibody reportedly stimulated adult hippocampal neurogenesis in a transgenic mouse model of AD (Biscaro et al., 2009). There are several differences between this and the current study that could explain the discrepant results, including mouse models and immunization procedures. It is noteworthy that 6 months of Aβ vaccination in the DKI mouse blocked the clustering of activated microglia around amyloid plaques but did not eliminate them from the dentate gyrus (Supplementary data), consistent with another report on the temporal responses of microglia to Aβ vaccination (Wilcock et al., 2001). Neuroinflammation is an established suppressor of adult hippocampal neurogenesis (Monje et al., 2003), and so the continuing presence of neuroinflammatory microglia in the dentate gyrus could contribute to the failure of vaccination to stimulate neurogenesis. Regardless of the mechanisms, our finding that exercise can restore hippocampal neurogenesis in the DKI mouse model of AD may be relevant to population-based studies that have associated increased physical activity with better cognitive performance in the elderly as well as individuals suffering from mild cognitive impairment (Laurin et al., 2001; Verghese et al., 2003; Geda et al., 2010). The contributions of impaired hippocampal neurogenesis and focal synapse loss to learning and memory deficits in the DKI mouse and the behavioral effects of rescuing each structural abnormality will require further study.

In summary, we have delineated both amyloid-dependent and -independent structural changes in the DKI mouse model of AD in the form of focal neuropil disruption and impaired hippocampal neurogenesis, respectively. Furthermore, we have identified a combination of amyloid-directed immunotherapy and voluntary exercise that blocks both the amyloid-dependent focal disruption of axons, dendrites and synapses as well as the amyloid-dissociated impairment in adult hippocampal neurogenesis. Combining an amyloid-directed immunotherapy or pharmacotherapy with physical exercise may be a strategy for achieving greater restoration of normal brain structure and neuroplasticity than can be obtained from either maneuver alone.

NIH-PA Author Manuscript

NIH-PA Author Manuscript

NIH-PA Author Manuscript

Supplementary Material

Refer to Web version on PubMed Central for supplementary material.

Acknowledgments

Supported by NIH grant AG17138 to R.S.

References

Auffret A, Gautheron V, Repici M, Kraftsik R, Mount HT, Mariani J, Rovira C. J. Neurosci. 2009; 29:144–152.

Biscaro B, Lindvall O, Hock C, Ekdahl CT, Nitsch RM. Abeta immunotherapy protects morphology and survival of adult-born neurons in doubly transgenic APP/PS1 mice. J. Neurosci. 2009; 29:14108–14119. [PubMed: 19906959]

Brendza RP, O'Brien C, Simmons K, McKeel DW, Bales KR, Paul SM, Olney JW, Sanes JR, Holtzman DM. PDAPP; YFP double transgenic mice: a tool to study amyloid-beta associated changes in axonal, dendritic, and synaptic structures. J. Comp. Neurol. 2003; 456:375–383. [PubMed: 12532409]

Buttini M, Masliah E, Barbour R, Grajeda H, Motter R, Johnson-Wood K, Khan K, Seubert P, Freedman S, Schenk D, Games D. Beta-amyloid immunotherapy prevents synaptic degeneration in a mouse model of Alzheimer's disease. J. Neurosci. 2005; 25:9096–9101. [PubMed: 16207868]

Chang KA, Suh YH. Pathophysiological roles of amyloidogenic carboxy-terminal fragments of the beta-amyloid precursor protein in Alzheimer's disease. J. Pharmacol. Sci. 2005; 97:461–471. [PubMed: 15821343]

Deng W, Saxe MD, Gallina IS, Gage FH. Adult-born hippocampal dentate granule cells undergoing maturation modulate learning and memory in the brain. J. Neurosci. 2009; 29:13532–13542. [PubMed: 19864566]

Donovan MH, Yazdani U, Norris RD, Games D, German DC, Eisch AJ. Decreased adult hippocampal neurogenesis in the PDAPP mouse model of Alzheimer's disease. J. Comp. Neurol. 2006; 495:70–83. [PubMed: 16432899]

Dupret D, Revest JM, Koehl M, Ichas F, De Giorgi F, Costet P, Abrous DN, Piazza PV. Spatial relational memory requires hippocampal adult neurogenesis. PLoS One. 2008; 3 e1959.

Flood DG, Lin YG, Lang DM, Trusko SP, Hirsch JD, Savage MJ, Scott RW, Howland DS. A transgenic rat model of Alzheimer's disease with extracellular Abeta deposition. Neurobiol. Aging. 2009; 30:1078–1090. [PubMed: 18053619]

Flood DG, Reaume AG, Dorfman KS, Lin YG, Lang DM, Trusko SP, Savage MJ, Annaert WG, De Strooper B, Siman R, Scott RW. FAD mutant PS-1 gene-targeted mice: increased A beta 42 and A beta deposition without APP overproduction. Neurobiol. Aging. 2002; 23:335–348. [PubMed: 11959395]

Games D, Bard F, Grejeda H, Guido T, Khan K, Soriano F, Vasquez N, Wehner N, Johnson-Wood K, Yednock T, Seubert P, Schenk D. Prevention and reduction of AD-type pathology in PDAPP mice immunized with A beta1-42. Ann. N.Y. Acad. Sci. 2000; 920:274–284. [PubMed: 11193164]

Games D, Buttini M, Kobayashi D, Schenk D, Seubert P. Mice as models: transgenic approaches and Alzheimer's disease. J. Alzheimers Dis. 2006; 9:133–149. [PubMed: 16914852]

Geda YE, Roberts RO, Knopman DS, Christianson TJ, Pankratz VS, Ivnik RJ, Boeve BF, Tangalos EG, Petersen RC, Rocca WA. Physical exercise, aging, and mild cognitive impairment: a population-based study. Arch. Neurol. 2010; 67:80–86. [PubMed: 20065133]

Gerdes J, Schwab U, Lemke H, Stein H. Production of a mouse monoclonal antibody reactive with a human nuclear antigen associated with cell proliferation. Int. J. Cancer. 1983; 31:13–20. [PubMed: 6339421]

Graeber MB, Streit WJ, Kreutzberg GW. Axotomy of the rat facial nerve leads to increased CR3 complement receptor expression by activated microglial cells. J. Neurosci. Res. 1988; 21:18–24. [PubMed: 3216409]

NIH-PA Author Manuscript

NIH-PA Author Manuscript

NIH-PA Author Manuscript

Gruntzendler J, Helmin K, Tsai J, Gan WB. Various dendritic abnormalities are associated with fibrillar amyloid deposits in Alzheimer's disease. Ann. N.Y. Acad. Sci. 2007; 1097:30–39. [PubMed: 17413007]

Hsia AY, Masliah E, McConlogue L, Yu GQ, Tatsuno G, Hu K, Kholodenko D, Malenka RC, Nicoll RA, Mucke L. Plaque-independent disruption of neural circuits in Alzheimer's disease mouse models. Proc. Natl. Acad. Sci. 1999; 96:3228–3233. [PubMed: 10077666]

Jack CR Jr, Knopman DS, Jagust WJ, Shaw LM, Aisen PS, Weiner MW, Petersen RC, Trojanowski JQ. Hypothetical model of dynamic biomarkers of the Alzheimer's Disease pathological cascade. Lancet Neurol. 2010; 9:119–128. [PubMed: 20083042]

Jin K, Galvan V, Xie L, Mao XO, Gorostiza OF, Bredesen DE, Greenberg DA. Enhanced neurogenesis in Alzheimer's disease transgenic (PDGF-APPSw,Ind) mice. Proc. Natl. Acad. Sci. 2004; 101:13363–13367. [PubMed: 15340159]

Johnson SA, Pasinetti GM, May PC, Ponte PA, Cordell B, Finch CE. Selective reduction of mRNA for the beta-amyloid precursor protein that lacks a Kunitz-type protease inhibitor motif in cortex from Alzheimer brains. Exp. Neurol. 1988; 102:264–268. [PubMed: 2460367]

Johnston JA, Froelich S, Lannfelt L, Cowburn RF. Quantification of presenilin-1 mRNA in Alzheimer's disease brains. FEBS Lett. 1996; 394:279–284. [PubMed: 8830658]

Kempermann G, van Praag H, Gage FH. Activity-dependent regulation of neuronal plasticity and self-repair. Prog. Brain Res. 2000; 127:35–48. [PubMed: 11142036]

Kitamura T, Saitoh Y, Takashima N, Murayama A, Niibori Y, Ageta H, Sekiguchi M, Sugiyama H, Inokuchi K. Adult neurogenesis modulates the hippocampus-dependent period of associative fear memory. Cell. 2009; 139:814–827. [PubMed: 19914173]

Knowles RB, Wyart C, Buldyrev SV, Cruz L, Urbanc B, Hasselmo ME, Stanley HE, Hyman BT. Plaque-induced neurite abnormalities: implications for disruption of neural networks in Alzheimer's disease. Proc. Natl. Acad. Sci. 1999; 96:5274–5279. [PubMed: 10220456]

Kolecki R, Lafauci G, Rubenstein R, Mazur-Kolecka B, Kaczmarski W, Frackowiak J. The effect of amyloidosis-beta and ageing on proliferation of neuronal progenitor cells in APP transgenic mouse hippocampus and in culture. Acta. Neuropathol. 2008; 116:419–424. [PubMed: 18483741]

Lanz TA, Carter DB, Merchant KM. Dendritic spine loss in the hippocampus of young PDAPP and Tg2576 mice and its prevention by the ApoE2 genotype. Neurobiol. Dis. 2003; 13:246–253. [PubMed: 12901839]

Laurin D, Verreault R, Lindsay J, MacPherson K, Rockwood K. Physical activity and risk of cognitive impairment and dementia in elderly persons. Arch Neurol. 2001; 58:498–504. [PubMed: 11255456]

Le R, Cruz L, Urbanc B, Knowles RB, Hsiao-Ashe K, Duff K, Irizarry MC, Stanley HE, Hyman BT. Plaque-induced abnormalities in neurite geometry in transgenic models of Alzheimer disease: implications for neural system disruption. J Neuropathol Exp Neurol. 2001; 60:753–758. [PubMed: 11487049]

Mann DM, Brown A, Wilks DP, Davies CA. Immunocytochemical and lectin histochemical studies of plaques and tangles in Down's syndrome patients at different ages. Prog Clin Biol Res. 1989; 317:849–856. [PubMed: 2532371]

Monje ML, Toda H, Palmer TD. Inflammatory blockade restores adult hippocampal neurogenesis. Science. 2003; 2302:1760–1765. [PubMed: 14615545]

Mouton, PR. Principles and Practices of Unbiased Stereology, An Introduction for Bioscientists. Baltimore: Johns Hopkins University Press; 2002.

Monsonego A, Maron R, Zota V, Selkoe DJ, Weiner HL. Immune hyporesponsiveness to amyloid beta-peptide in amyloid precursor protein transgenic mice: implications for the pathogenesis and treatment of Alzheimer's disease. Proc Natl Acad Sci. 2001; 98:10273–10278. [PubMed: 11517335]

Morgan D. Immunotherapy for Alzheimer's disease. J Alzheimer's Dis. 2006; 9:425–432.

Morris JC, Price AL. Pathologic correlates of nondemented aging, mild cognitive impairment, and early-stage Alzheimer's disease. J Mol Neurosci. 2001; 17:101–118. [PubMed: 11816784]

NIH-PA Author Manuscript

NIH-PA Author Manuscript

NIH-PA Author Manuscript

Mucke L, Masliah E, Johnson WB, Ruppe MD, Alford M, Rockenstein EM, Forss-Petter S, Pietropaolo M, Mallory M, Abraham CR. Synaptotrophic effects of human amyloid beta protein precursors in the cortex of transgenic mice. Brain Res. 1994; 666:151–167. [PubMed: 7882025]

Nacher J, Crespo C, McEwen BS. Doublecortin expression in the adult rat telencephalon. Eur J Neurosci. 2001; 14:629–644. [PubMed: 11556888]

Nalbantoglu J, Tirado-Santiago G, Lahsaïni A, Poirier J, Goncalves O, Verge G, Momoli F, Welner SA, Massicotte G, Julien JP, Shapiro ML. Impaired learning and LTP in mice overexpressing the carboxy terminus of the Alzheimer amyloid precursor protein. Nature. 1997; 387:500–505. [PubMed: 9168112]

Naumann N, Alpár A, Ueberham U, Arendt T, Gartner U. Transgenic expression of human wild-type amyloid precursor protein decreases neurogenesis in the adult hippocampus. Hippocampus. 2009 Aug 27. [Epub ahead of print]; PMID 19714567.

Rao MS, Shetty AK. Efficacy of doublecortin as a marker to analyse the absolute number and dendritic growth of newly generated neurons in the adult dentate gyrus. Eur J Neurosci. 2004; 19:234–246. [PubMed: 14725617]

Reaume AG, Howland DS, Trusko SP, Savage MJ, Lang DM, Greenberg BD, Siman R, Scott RW. Enhanced amyloidogenic processing of the beta-amyloid precursor protein in gene-targeted mice bearing the Swedish familial Alzheimer's disease mutations and a "humanized" Abeta sequence. J Biol Chem. 1996; 271:23380–23388. [PubMed: 8798542]

Rockenstein EM, McConlogue L, Tan H, Power M, Masliah E, Mucke L. Levels and alternative splicing of amyloid beta protein precursor (APP) transcripts in brains of APP transgenic mice and humans with Alzheimer’s disease. J Biol Chem. 1995; 270:28257–28267. [PubMed: 7499323]

Savage MJ, Iqbal M, Loh T, Trusko SP, Scott R, Siman R, Cathepsin G. Localization in human cerebral cortex and generation of amyloidogenic fragments from the beta-amyloid precursor protein. Neuroscience. 1994; 60:607–619. [PubMed: 7936190]

Siman R, Flood DG, Thinakaran G, Neumar RW. Endoplasmic reticulum stress-induced cysteine protease activation in cortical neurons: effect of an Alzheimer's disease-linked presenilin-1 knock-in mutation. J Biol Chem. 2001; 276:44736–44743. [PubMed: 11574534]

Siman R, Reaume AG, Savage MJ, Trusko S, Lin YG, Scott RW, Flood DG. Presenilin-1 P264L knock-in mutation: differential effects on abeta production, amyloid deposition, and neuronal vulnerability. J Neurosci. 2000; 20:8717–8726. [PubMed: 11102478]

Siman R, Salidas S. Gamma-secretase subunit composition and distribution in the presenilin wild-type and mutant mouse brain. Neuroscience. 2004; 129:615–628. [PubMed: 15541883]

Spires TL, Meyer-Luehmann M, Stern EA, McLean PJ, Skoch J, Nguyen PT, Bacskai BJ, Hyman BT. Dendritic spine abnormalities in amyloid precursor protein transgenic mice demonstrated by gene transfer and intravital multiphoton microscopy. J Neurosci. 2005; 25:7278–7287. [PubMed: 16079410]

Sternberger LA, Sternberger NH. Monoclonal antibodies distinguish phosphorylated and nonphosphorylated forms of neurofilaments in situ. Proc Natl Acad Sci. 1983; 80:6126–6130. [PubMed: 6577472]

Terry RD, Masliah E, Salmon DP, Butters N, DeTeresa R, Hill R, Hansen LA, Katzman R. Physical basis of cognitive alterations in Alzheimer's disease: synapse loss is the major correlate of cognitive impairment. Ann Neurol. 1991; 30:572–580. [PubMed: 1789684]

Thinakaran G, Borchelt DR, Lee MK, Slunt HH, Spitzer L, Kim G, Ratovitsky T, Davenport F, Nordstedt C, Seeger M, Hardy J, Levey AI, Gandy SE, Jenkins NA, Copeland NG, Price DL, Sisodia SS. Endoproteolysis of presenelin 1 and accumulation of processed derivatives in vivo. Neuron. 1996; 17:181–190. [PubMed: 8755489]

Tsai J, Grutzendler J, Duff K, Gan WB. Fibrillar amyloid deposition leads to local synaptic abnormalities and breakage of neuronal branches. Nat Neurosci. 2004; 7:1181–1183. [PubMed: 15475950]

van Praag H, Kempermann G, Gage FH. Running increases cell proliferation and neurogenesis in the adult mouse dentate gyrus. Nat Neurosci. 1999; 2:266–270. [PubMed: 10195220]

NIH-PA Author Manuscript

NIH-PA Author Manuscript

NIH-PA Author Manuscript

Verghese J, Lipton RB, Katz MJ, Hall CB, Derby CA, Kuslansky G, Ambrose AF, Sliwinski M, Buschke H. Leisure activities and the risk of dementia in the elderly. N Engl J Med. 2003; 348:2508–2516. [PubMed: 12815136]

Verret L, Jankowsky JL, Xu GM, Borchelt DR, Rampon C. Alzheimer's type amyloidosis in transgenic mice impairs survival of newborn neurons derived from adult hippocampal neurogenesis. J Neurosci. 2007; 27:6771–6780. [PubMed: 17581964]

Wen PH, Shao X, Shao Z, Hof PR, Wisniewski T, Kelley K, Friedrich VL Jr, Ho L, Pasinetti GM, Shoji J, Robakis NK, Elder GA. Overexpression of wild type but not an FAD mutant presenilin-1 promotes neurogenesis in the hippocampus of adult mice. Neurobiol Dis. 2002; 10:8–19. [PubMed: 12079399]

Wilcock DM, Colton CA. Anti-amyloid-beta immunotherapy in Alzheimer's disease: relevance of transgenic mouse studies to clinical trials. J Alzheimers Dis. 2008; 15:555–569. [PubMed: 19096156]

Wilcock DM, Gordon MN, Ugen KE, Gottschall PE, Di Carlo G, Dickey C, Boyett KW, Jantzen PT, Connor KE, Melachrino J, Hardy J, Morgan D. Number of Abeta innoculations in APP1 transgenic mice influences antibody titers, microglial activation, and congophilic plaque levels. DNA Cell Biol. 2001; 20:731–736. [PubMed: 11788051]

Zhang C, McNeil E, Dressler L, Siman R. Long-lasting impairment in hippocampal neurogenesis associated with amyloid deposition in a knock-in mouse model of familial Alzheimer's disease. Exp Neurol. 2007; 204:77–87. [PubMed: 17070803]

NIH-PA Author Manuscript

NIH-PA Author Manuscript

NIH-PA Author Manuscript

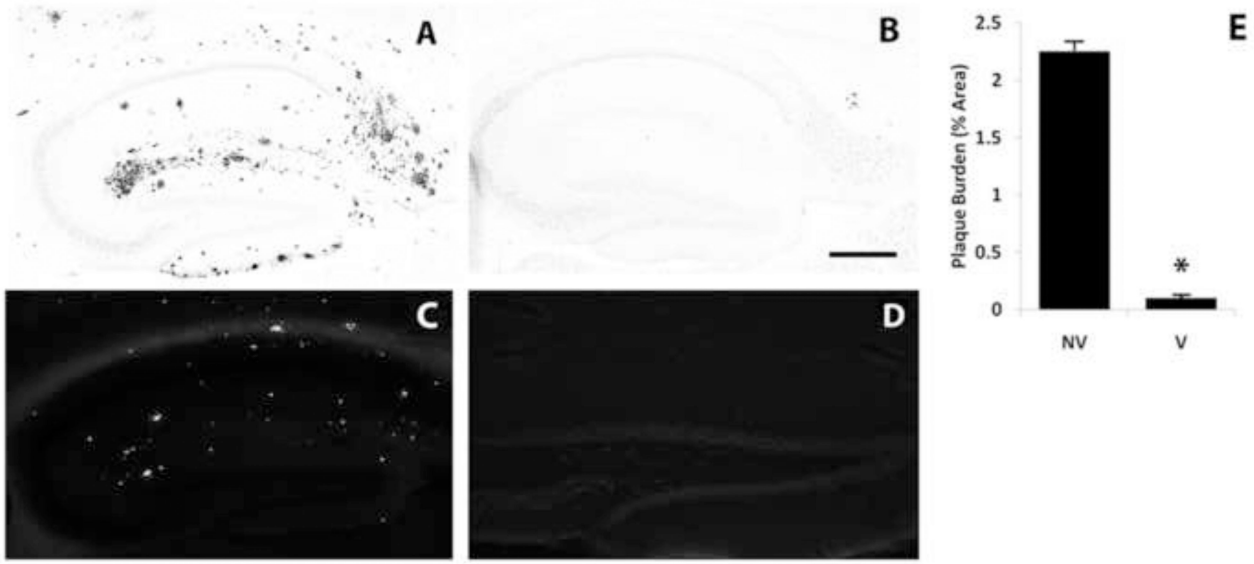

Figure 1.

Near-complete blockade of hippocampal amyloid deposition by Aβ vaccination. Sagittal sections through the dorsal hippocampus of 14-month-old DKI mice were immunostained for Aβ (A, B) or labeled with thioflavin S (C, D) without treatment (A,C; NV, n=17) or six months after initiating Aβ vaccination (B,D; V, n=16). (E) Quantitative morphometric analysis of the blockade of amyloid deposition. Scale bar= 500 μm. *p<.001.

NIH-PA Author Manuscript

NIH-PA Author Manuscript

NIH-PA Author Manuscript

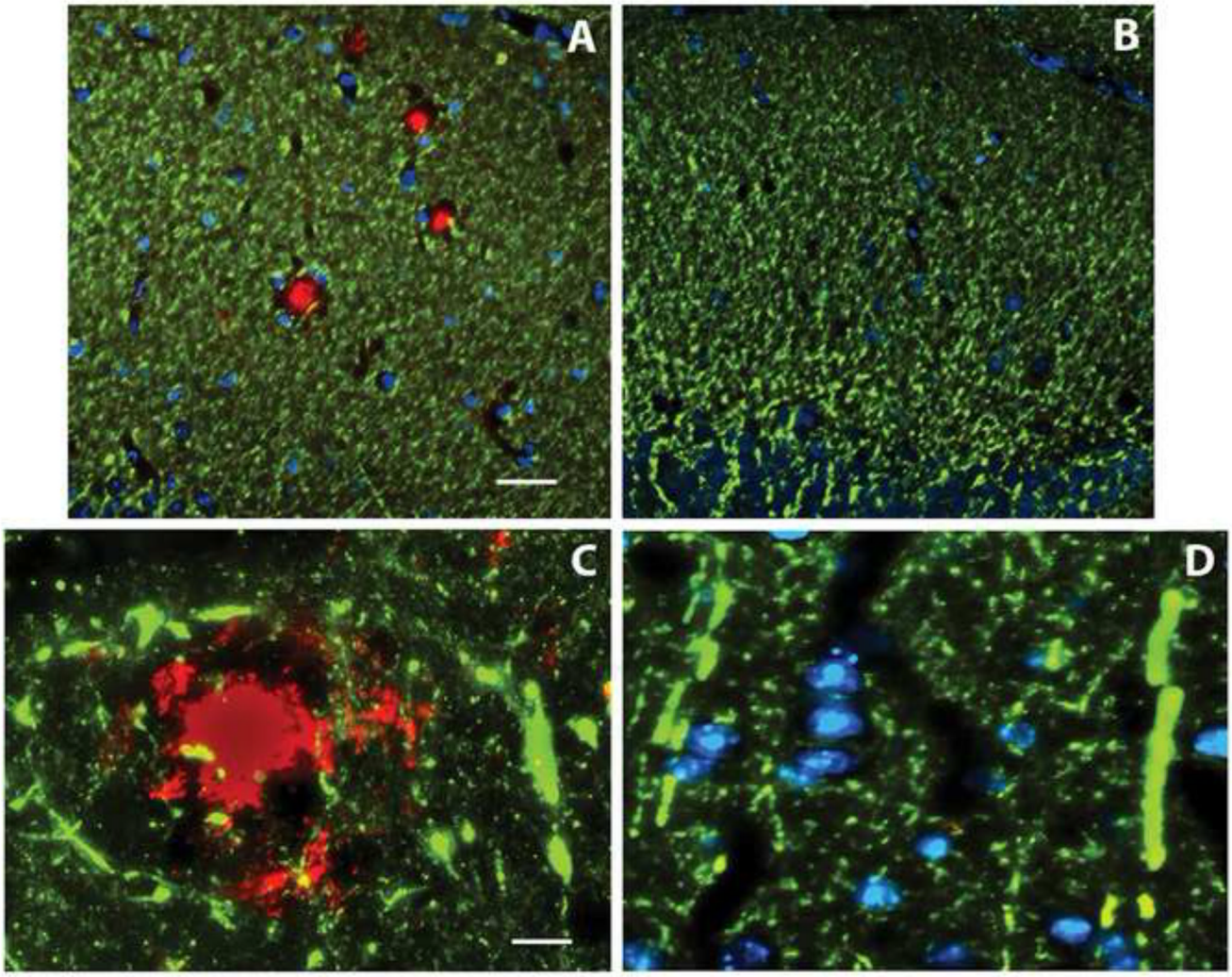

Figure 2.

Loss and dysmorphology of dendrites is confined to amyloid plaques. MAP2 immunostaining (green) of the dentate molecular layer (A,B) and parietal neocortex (C,D) of the 14 month old DKI mouse either not receiving treatment (A,C) or six months after initiating Aβ vaccination (B,D). Panel A illustrates that the dense dendritic network is interrupted by spheres that immunolabel for Aβ (red). Neither amyloid deposits nor gaps in the dendritic network are observed following Aβ vaccination (B). Nuclei labeled with DAPI are shown in blue. At high magnification, amyloid deposits are surrounded by curvy dendrites (C). This abnormal dendritic morphology is not found following Aβ vaccination (D). Scale bar= 50 μm (A,B); 10 μm (C,D).

NIH-PA Author Manuscript

NIH-PA Author Manuscript

NIH-PA Author Manuscript

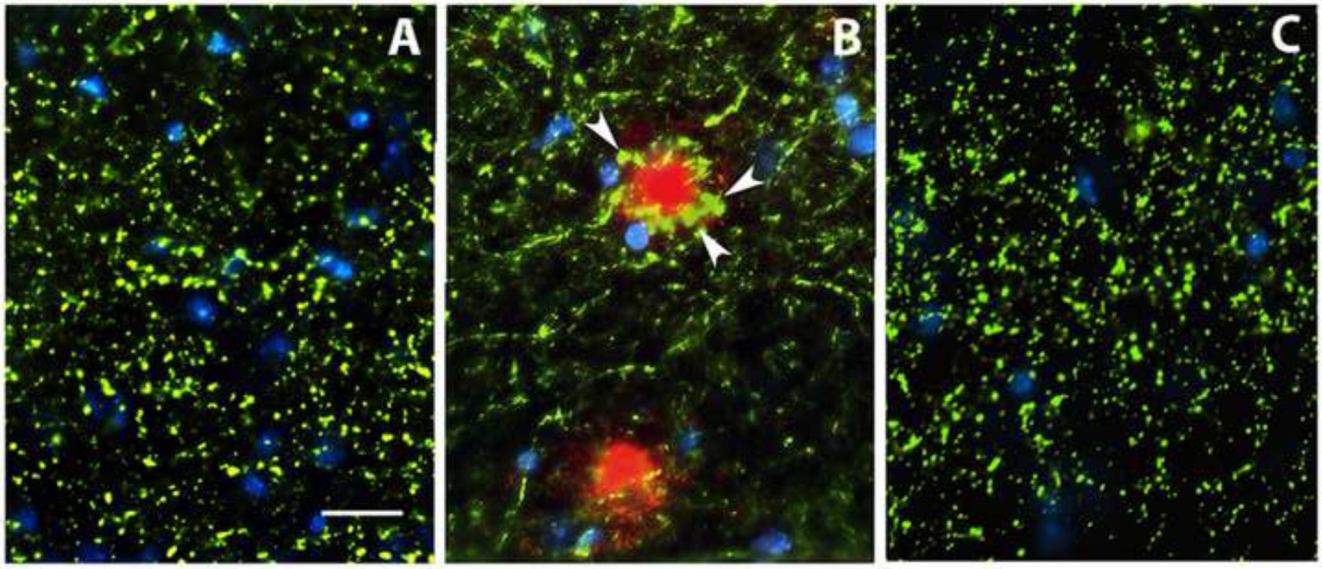

Figure 3.

Axonal loss and dystrophy are confined to amyloid plaques. pNFH immunostaining of the dentate molecular layer of 14 month old mice either wild type (A), DKI (B), or DKI six months after initiating Aβ vaccination (C). In (A), cross-sectioned axons appear as small spheres (green). Areas with amyloid deposition (red) are depleted of the small axonal spheres, and at their periphery have clusters of swollen varicosities indicative of dystrophic axons (B, arrowheads). Aβ vaccination blocks the focal loss of immunostained axons and the accumulation of swollen varicosities (C). Nuclei are stained with DAPI (blue). Scale bar= 20 μm.

NIH-PA Author Manuscript

NIH-PA Author Manuscript

NIH-PA Author Manuscript

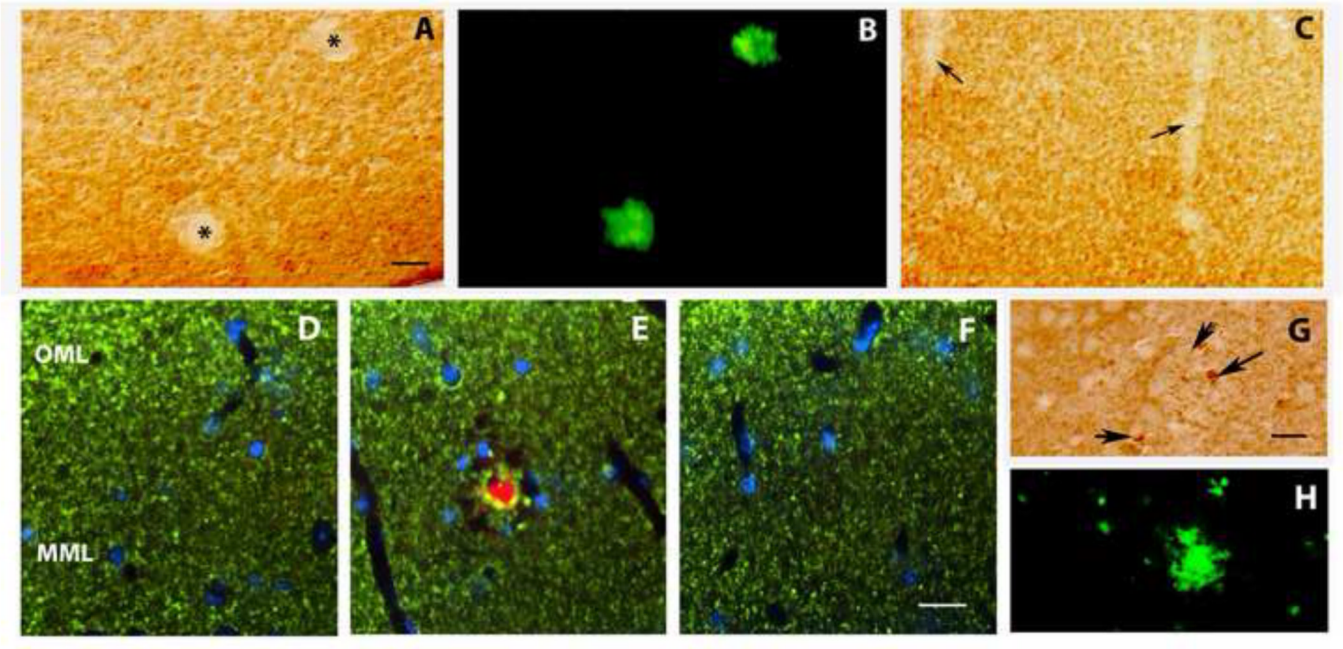

Figure 4.

Synapse loss is confined to amyloid plaques. Immunostaining of dendritic spines for spinophilin (A,C), pre-synaptic terminals for synaptophysin (D–G), and staining of fibrillar amyloid plaques with thioflavin S (B,H). Note in panel A that immunostained puncta indicative of dendritic spines are dispersed throughout the dentate molecular layer of the DKI mouse, except in discrete spheres (asterisks) that co-localize for amyloid deposits (B, green). Following six months of Aβ vaccination, spine-depleted spheres are no longer observed, and the dispersed network of spines is interrupted only by blood vessels traversing the molecular layer (C, arrows). Similarly, the dentate molecular layer of the wild-type mouse contains dispersed puncta of synaptophysin immunoreactivity indicative of nerve terminals (D, green). In DKI mice, the nerve terminal network is interrupted by spheres that are depleted of terminals and co-stain for amyloid (red), and the amyloid deposits are surrounded by swollen, enlarged terminals (E). Aβ vaccination eliminates both the spheres depleted of nerve terminals and the terminal swellings (F). Nuclei stained with DAPI are shown in blue. (G,H) Double staining for synaptophysin and thioflavin S confirmed that the nerve terminal swellings (G, arrows) are associated with fibrillar amyloid plaques (H). Scale bar= 20 μm.

NIH-PA Author Manuscript

NIH-PA Author Manuscript

NIH-PA Author Manuscript

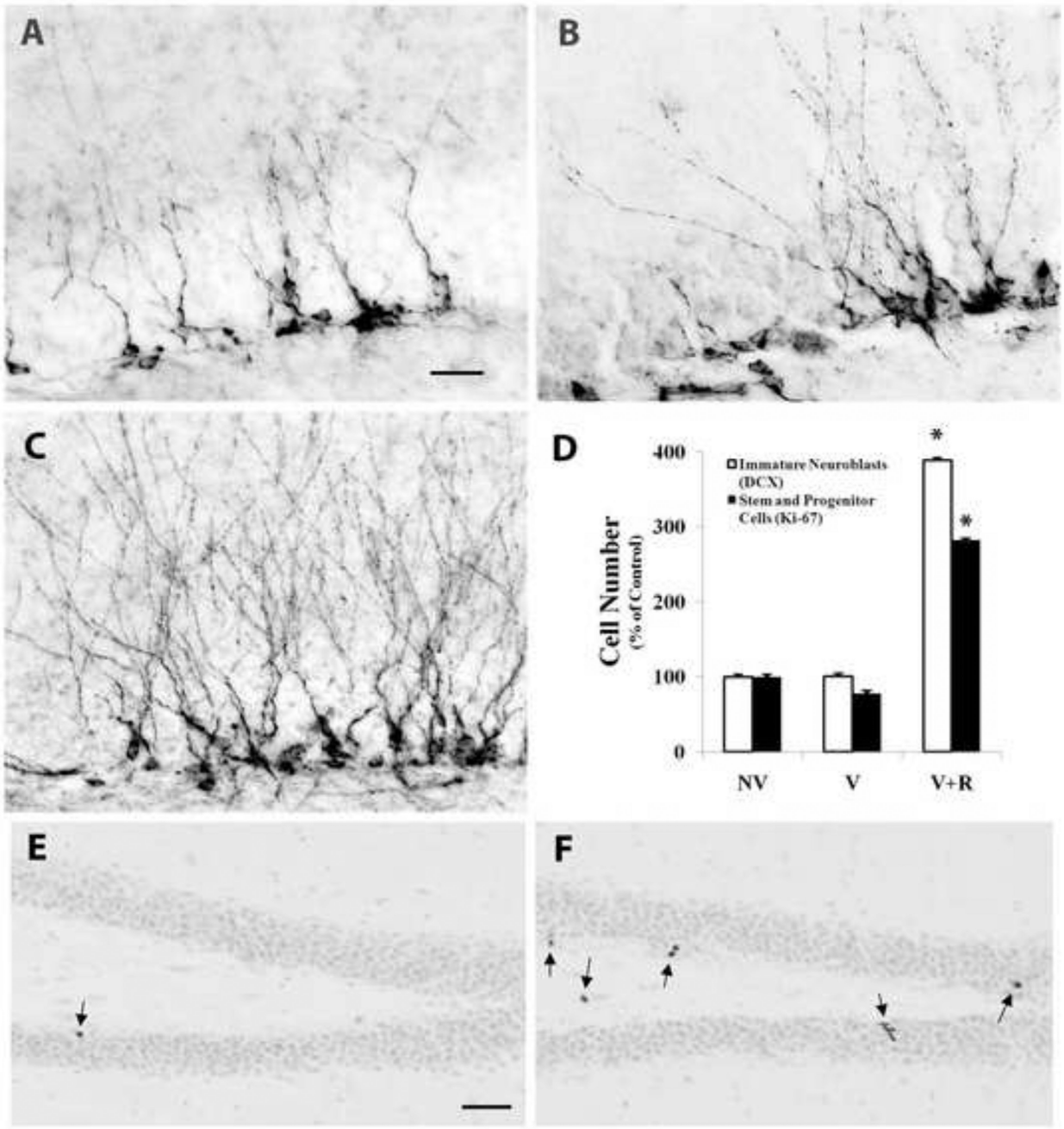

Figure 5.

Hippocampal neurogenesis is not altered by Aβ vaccination but is stimulated when the vaccine is combined with physical exercise. (A–C) Sagittal sections through dorsal hippocampus immunostained for the immature neuronal marker doublecortin. The numbers of immature neurons were comparable between DKI mice either untreated (A; NV, n=20) or vaccinated with Aβ (B; V, n=14). In contrast, the addition of wheel running exercise to the Aβ vaccination led to a marked increase in the number of immature neurons as well as the density of their dendritic arborizations (C; V+R, n=9). The addition of exercise to the Aβ vaccination also increased markedly the number of nuclei in the subgranular zone immunopositive for the dividing neural progenitor marker Ki-67 (compare E, nonvaccinated

NIH-PA Author Manuscript

NIH-PA Author Manuscript

NIH-PA Author Manuscript

(NV, n=8) with F, vaccinated plus running (V+R, n=9). The arrows denote dividing Ki-67-positive neural progenitors. E and F are lightly counterstained with hematoxylin to illustrate the location of Ki-67-positive nuclei in the subgranular zone. D – quantitative analysis of immature neuron and dividing neural progenitor cell numbers in the subgranular zone of DKI mice receiving either no treatment (NV), vaccination (V), or vaccination combined with exercise (V+R). Scale bar= 20 μm (A–C); 100μm (E,F). *p<.002.

NIH-PA Author Manuscript

NIH-PA Author Manuscript

NIH-PA Author Manuscript

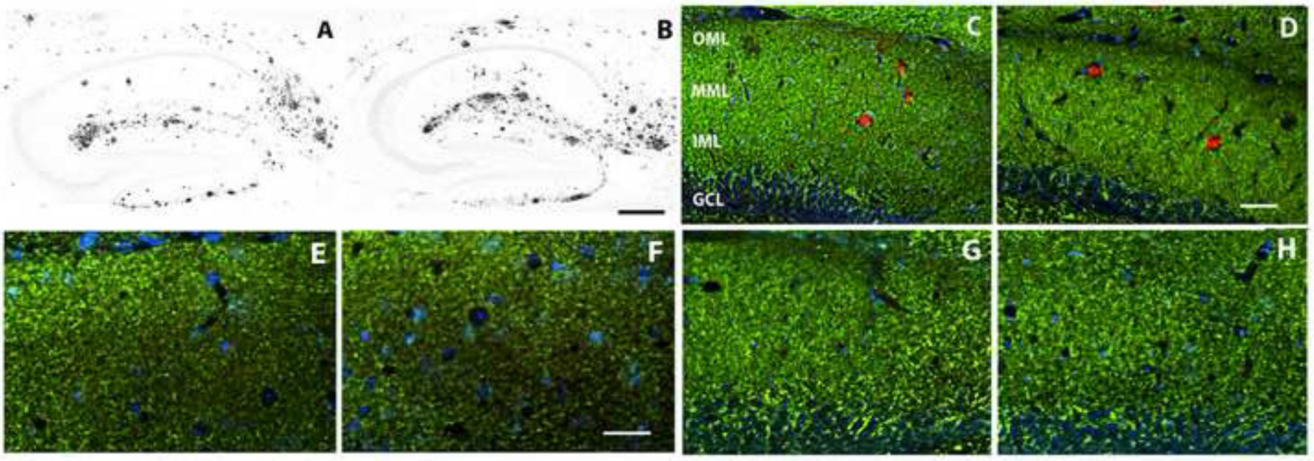

Figure 6.

Combining exercise with Aβ vaccination does not interfere with the restorative effects of the vaccine on forebrain neuropil, whereas exercise alone is ineffective. (A–D) A 30 period of voluntary exercise does not appreciably alter hippocampal amyloid deposition (A: DKI sedentary; B: DKI after wheel running), or amyloid-dependent dendritic disruption in dentate molecular layer (C: DKI sedentary; D: DKI after wheel running). (E–H) Effects of combination therapy on the neuropil. The dentate molecular layer immunostained for synaptophysin (E,F) or MAP2 (C,D,G,H). (E,G) wild type; (F,H) DKI after vaccination plus wheel running. Note that the density of immunostained nerve terminals and dendrites do not differ appreciably between wild type mice and DKI mice receiving the combination therapy. Scale bar= 500 μm (A,B); 50 μm (C–H). Abbreviations: OML- outer molecular layer; MML- middle molecular layer; IML-inner molecular layer; GCL- granule cell layer.